The International Journal of Advanced Manufacturing Technology (2019) 101:367–375
https://doi.org/10.1007/s00170-018-2917-6

ORIGINAL ARTICLE

Experimental and simulation study on micro hole machining in EDM with high-speed tool electrode rotation

Guanglei Feng[1] · Xiaodong Yang[1] · Guanxin Chi[1]

Received: 14 June 2018 / Accepted: 22 October 2018 / Published online: 1 November 2018

Abstract

In order to improve the machining characteristics, rotational electrode has been widely used in machining micro holes in electrical discharge machining (EDM). In the current work, a high spindle speed EDM was employed for machining holes, and the effect of the rotating speed on the material removal rate, electrode wear, and the taper of the hole was studied. Fluent software was used to simulate the flow field of the working gap medium at different rotating speeds of the tool electrode, and the velocity field of the working gap medium and the distribution of the discharge debris particles in the working gap at different rotating speeds of the tool electrode were investigated. The results show that increasing the rotating speed of the tool electrode brings higher removal rate and lower electrode wear and taper of the hole. This is because increasing the rotating speed of the tool electrode can promote the flow velocity of the working gap flow field, and the efflux velocity of working liquid containing discharge debris particles is speeded up.

Keywords Micro electrical discharge machining · Non-contact electric feeding · High electrode rotational speed · Material removal rate · Electrode wear

1 Introduction

With the development of aeronautics and astronautics, the demands of the fuel injection system of aero-engine and the blade air film cooling holes are increasing [1, 2]. Electrical discharge machining (EDM) is one of the common methods of micro hole machining. However, with the increase of the machining depth of the micro holes, the discharge debris particles produced in the process cannot be removed from the working gap in time. It is easy to cause localized discharge or even short circuit, resulting in difficult processing. In order to improve the machining performance of micro holes in EDM, the removal efficiency of the discharge debris particles in micro hole machining must be improved. At present, researchers have adopted many methods to promote the removal efficiency of the discharge debris particles, such as the combination of electrode rotation, ultrasonic vibration auxiliary, electrode jump motion, or the injection and suction flushing method using tubular electrode [3].

Soni et al. [4] and Cyril et al. [5] conducted micro hole machining using the rotating tool electrode in micro EDM. The results showed that the tool electrode rotation could improve the material removal rate significantly. However, the tool electrode rotational speed used in the above study was limited to hundreds of revolutions per minute. Tong et al. [6] and Zhang et al. [7, 8] introduced the ultrasonic vibration to the workpiece in micro drilling EDM, which improves the material removal rate. But the micro-amplitude vibration of the workpiece was realized by applying high-frequency sine-wave voltage to drive a piezoelectric (PZT) actuator, which increased the complexity of the device. Masuzawa and Heuvelman [9] studied the electrode jump motion in micro drilling EDM. The results showed that using the electrode jump could improve the speed of the medium fluid in the gap. But the frequent electrode jump in unit time would reduce the discharge time. The injection and suction flushing method using tubular electrode [10, 11] can make the medium of the working gap flow faster. However, micro EDM is based on micro electrodes, and considering the limits of its electrode's scale, these methods could not be used in micro EDM when the diameter of the electrode was less than dozens of microns.

✉ Xiaodong Yang
xdyang@hit.edu.cn

[1] School of Mechatronics Engineering, Harbin Institute of Technology, Harbin, China

Some researchers [12–15] used flatted electrode, helical electrode, or other special-shaped electrodes in combination with electrode rotation in micro hole machining. Through these measures, the removal of the discharge debris particles, which will improve the stability of the discharge state and achieve a higher machining speed, can be promoted. However, it takes a lot of time to machine the special-shaped electrode itself, resulting in a decrease in productivity.

Zhang et al. [16] studied the effect of tool electrode rotational speed on the machining efficiency. The results showed that the machining efficiency increased as the spindle rotational speed increased. Since the power supply brush on, the spindle increased the vibration and the wear of the spindle at higher spindle speeds; the maximum speed used in the study was only at 15000 rpm. However, the vibration caused by the contact of the brush with the rotating spindle will have a certain influence on EDM. Therefore, this experimental result cannot be completely considered as a pure evaluation of the influence of the spindle rotational speed.

In this paper, a micro EDM method using non-contact electric feeding based on the principle of electrostatic induction feeding method [17–19] is used to realize the non-contact feeding to the tool electrode. It makes no contact point and force on the spindle, which can ensure that the spindle rotation accuracy is always stable. In order to determine the influence of the high rotational speed of the tool electrode on the machining characteristics of micro holes, a micro hole machining experiment with different depth was carried out at different rotational speeds of the tool electrode. In order to explain the influence of the rotating speed of the tool electrode on the machining characteristics, the simulation model of the working gap medium at different rotating speeds of the tool electrode was established. In addition, the velocity field of the working gap medium and the distribution of the discharge debris in the working gap at different rotating speeds of the tool electrode were analyzed.

2 Micro hole machining with high spindle speed

2.1 Experimental equipment

Micro EDM using non-contact electric feeding is based on the principle of electrostatic induction feeding method. Figure 1 shows the equivalent circuit of micro EDM using electrostatic induction feeding method. It consists of a pulse power supply V, a feeding capacitance C_1, and a working gap equivalent capacitance C_2. During the electrical discharge machining, charge transfer occurs between the feeding capacitance C_1 and working gap equivalent capacitance C_2 [17].

Figure 2 shows the high spindle speed micro EDM system [20]. The tool electrode was fixed to the tool electrode holder

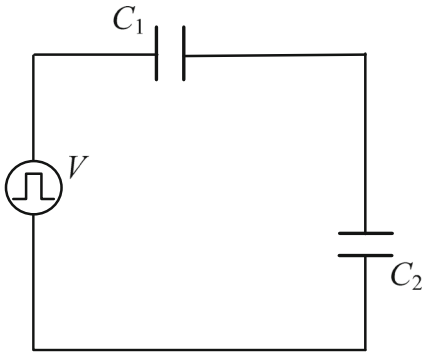

Fig. 1 Equivalent circuit of micro EDM using electrostatic induction feeding method [17]

which was held by the chuck of the motorized spindle (EM30-S6000 of NSK). The tool electrode holder was electrically isolated from the spindle by an insulation pipe and rotated with a rotational speed up to 60,000 rpm. Non-contact electric feeding to the tool electrode was realized using the electrostatic induction feeding method. A cylindrical feeding electrode was aligned coaxially to the tool electrode holder to form a capacitance C_1 in between.

Furthermore, a ring-shaped non-contact voltage probe was installed coaxially to the tool electrode holder in a similar manner to the feeding electrode as shown in Fig. 1. This is because drilling was difficult with constant feed speeds of the tool electrode. To avoid short circuiting, the working gap voltage was measured by the non-contact measuring method to control the gap width using a newly developed servo feed control system [20].

2.2 Preparation of micro electrodes

There are mainly two methods to machine micro electrode online, wire electrical discharge grinding (WEDG) and block electrical discharge grinding (BEDG). A larger discharge area in BEDG leads to the larger capacitance between the tool electrode and the block electrode, which can obtain lower

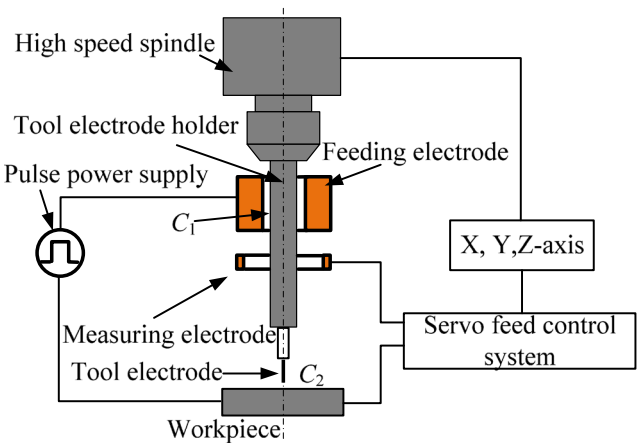

Fig. 2 Experimental setup

working gap voltage according to the principle of the capacity coupling. So, it is beneficial to machining micro electrodes with this method.

Figure 3 shows BEDG using non-contact electric feeding method. In the experiment, the block electrode was fixed on the tank and the tool electrode did servo feed/back motion in x direction. Figure 4 shows the micro rod machined by BEDG under conditions shown in Table 1.

2.3 Experimental method

Micro holes were drilled on a tool steel plate with thickness of 20 μm, 100 μm, and 200 μm. The diameter of the tool electrode was Φ164–167 μm, which was prepared by BEDG. Machining conditions were shown in Table 2.

2.4 Experimental results and analysis

2.4.1 Influence of rotating speed of tool electrode on material removal rate

The material removal rate was obtained by dividing the volume of the hole by the machining time. Figure 5 shows the relationship between the rotating speed of the tool electrode and the material removal rate. It can be seen that the material removal rate improves as the rotating speed of the tool electrode increases. The material removal rate with 20-μm depth of hole is greater than that with 200-μm depth of hole. This is because when the depth of the hole is 20 μm, the discharge debris particles hardly accumulate in the working gap due to the flushing. Under the regulation of the servo control system, it can always be in a good discharge state. When the depth of the hole was 20 μm, the growth rate of the material removal rate gradually decreased with the increase of the rotating speed

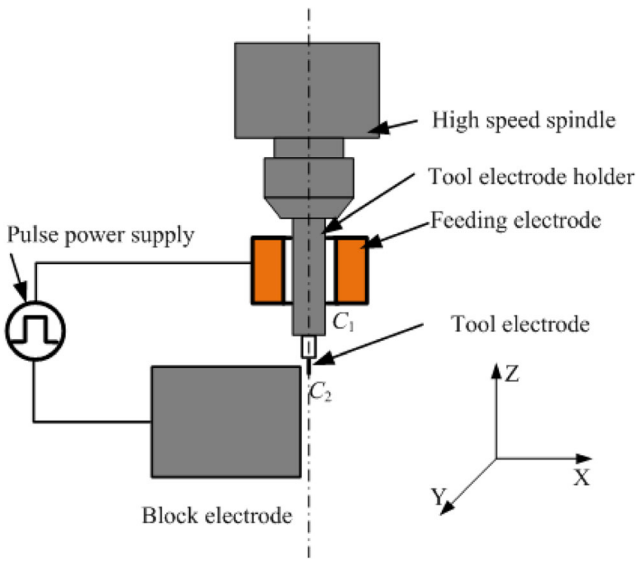

Fig. 3 BEDG using non-contact electric feeding method

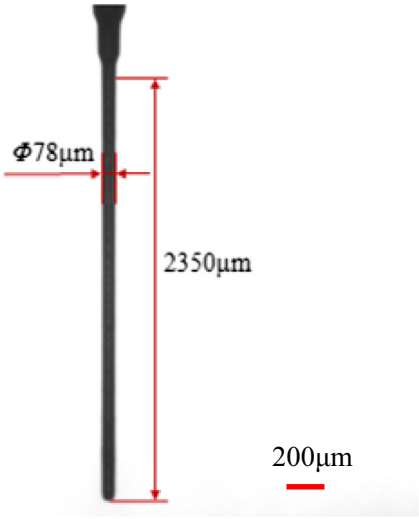

Fig. 4 Micro rod machined by BEDG with spindle rotational speeds of 60,000 rpm

of the tool electrode. However, when the depth of the hole was 100 μm or 200 μm, the growth rate of the material removal rate increased with the increase of the rotating speed of the tool electrode. In addition, when the depth of the hole is 200 μm, the material removal rate at the tool electrode rotational speed of 60,000 rpm is 6.3 times higher than that at 1000 rpm. However, when the depth of the hole is 100 μm, the material removal rate at the tool electrode rotational speed of 60,000 rpm is only 2.2 times higher than that at 1000 rpm. Therefore, the higher rotating speed of the tool electrode has a better effect on improving the material removal rate during deeper hole machining.

2.4.2 Influence of rotating speed of tool electrode on electrode wear

The electrode wear ratio was obtained by dividing the electrode volumetric wear by the workpiece volumetric removal in unit time. Figure 6 shows the influence of the rotating speed of the tool electrode on the electrode wear ratio with different depth of the hole. It can be seen that when the depth of the hole is 20 μm, the increase of the rotating speed of the tool electrode has little improvement in electrode wear ratio. When the

Table 1 Experimental conditions

Parameter	Value
Amplitude (V)	400
Frequency (MHz)	2
Duty factor (%)	50
Feeding capacitance C_1 (pF)	13
Spindle speed (rpm)	60,000
Feed speed (μm/s)	0.3–0.6
Dielectric	EDM-oil

Table 2 Experimental conditions

Parameter	Value
Amplitude (V)	400
Frequency (MHz)	2
Duty factor (%)	50
Feeding capacitance C_1 (pF)	13
Spindle speed (rpm)	1000–60,000
Workpiece	Tool steel
Feed speed (μm/s)	3
Dielectric	EDM-oil

depth of the hole is 100 μm or 200 μm, the electrode wear ratio decreases with the increase of the rotating speed of tool electrode. The deeper the hole is, the more effective the reduction of the electrode wear ratio by increasing the rotating speed of the tool electrode is.

2.4.3 Influence of rotating speed of tool electrode on taper of micro hole

Figure 7 shows the inlet and outlet of micro holes at different tool electrode rotation. The inlets of the machined holes with the rotating speed of 1000 rpm and 60,000 rpm are shown in Fig. 7a and c, and the outlets are shown in Fig. 7b and d, respectively. It can be seen that the diameter of the inlet obtained by the rotating speed of 1000 rpm is larger than that of the inlet obtained by the rotating speed of 60,000 rpm. However, when the spindle speed is 1000 rpm, the diameter of the outlet obtained by the rotating speed of 1000 rpm is smaller than that of the inlet obtained by the rotating speed of 60,000 rpm.

Figure 8 shows the diameter of the machined holes at the speed of 1000 rpm and 60,000 rpm, respectively. When the rotating speed is 1000 rpm, the diameter of the inlet is 6.26 μm

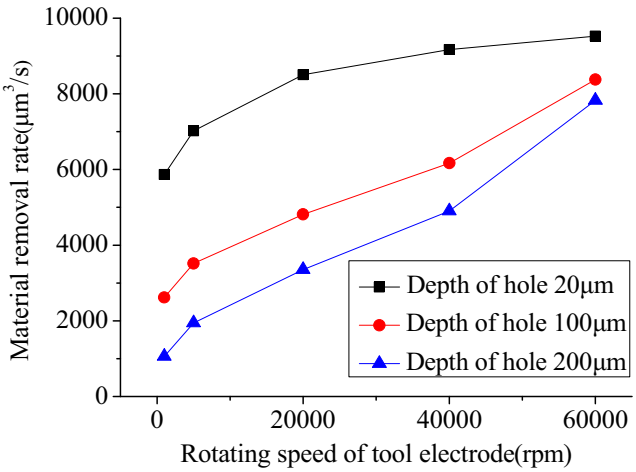

Fig. 5 Relationship between rotating speed of tool electrode and material removal rate

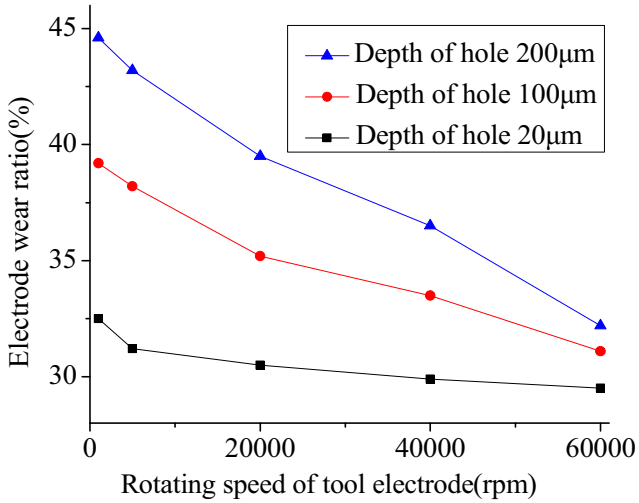

Fig. 6 Influence of rotating speed of tool electrode on electrode wear ratio with different depth of hole

larger than the diameter of the outlet, and the taper of the hole is about 0.067. While the rotating speed is 60,000 rpm, the diameter of the inlet is 4 μm larger than the diameter of the outlet, and the taper of the hole is only 0.04. Higher rotating speed of the tool electrode can get micro holes with smaller taper. So the machining accuracy of the holes obtained at high spindle speed is better.

3 Simulation analysis of working gap flow field

In order to clarify the specific reasons that the material removal rate, electrode wear, and taper of the hole can be improved by increasing the rotating speed of the tool electrode in micro hole machining, a working gap flow field was simulated. The effects of the rotating speed of the tool electrode on the working gap flow field and the distribution of discharge debris particles in the working gap were analyzed.

3.1 Establishment of simulation model

The geometric model of micro hole machining with high electrode rotational speed is shown in Fig. 9. The figure shows the geometric relationship among the high-speed rotating electrode, the workpiece, the working fluid medium, and the way of the flushing liquid. It is assumed that the working fluid enters from the nozzle and flows out from the outlet of the medium.

3.2 Mathematical model of fluid

The following assumptions are made for the working gap flow field in this paper: (1) the working gap fluid is an incompressible continuous medium, (2) when the flow field is stable, the

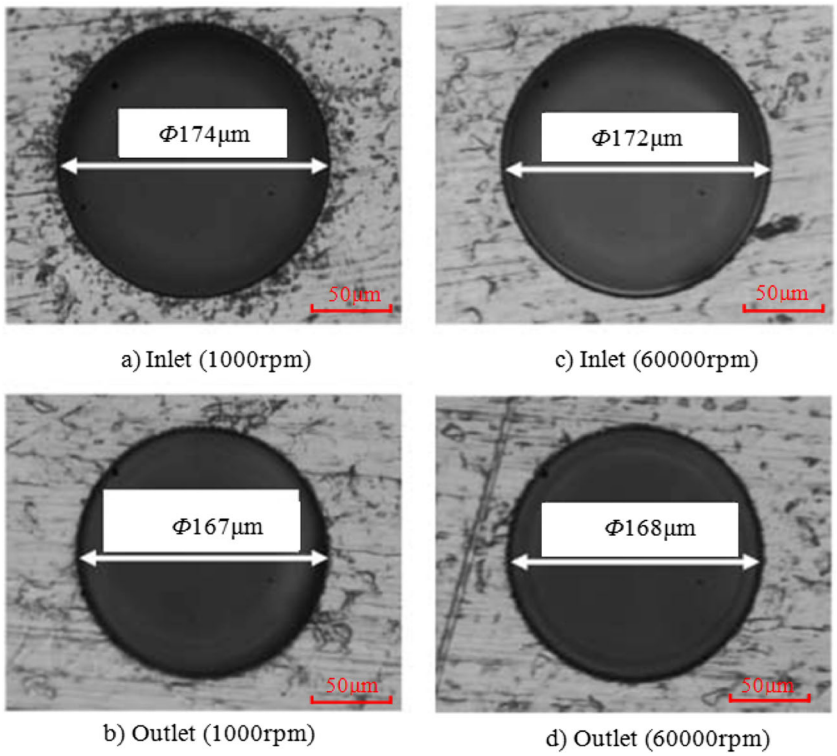

Fig. 7 Inlet and outlet of micro holes at different tool electrode rotation

physical quantities of the flow field are only related to the spatial coordinates but not to the time, (3) considering the effect of liquid and electrode rotation, the heat generated by the discharge is easier to disperse, so the influence of temperature field on the flow field is neglected. Based on the above assumptions, the continuity equation and momentum conservation equation of the working gap fluid in micro hole machining are established.

$$\nabla V = 0 \tag{1}$$

$$\rho \frac{\mathrm{d}V}{\mathrm{d}t} = \rho F - \nabla p + \mu \Delta V \tag{2}$$

where, ∇ is a vector differential operator, V is the velocity of the fluid, ρ is the density of the fluid, μ is fluid viscosity, F is the volume force, P is the fluid pressure coefficient, and Δ is the Laplace operator.

3.3 Model of discharge debris particles

The discharge debris particles in the working gap were affected by the working gap fluid, and their motion followed Newton's second law. The motion equation of the discharge debris particles is expressed as,

$$\frac{\mathrm{d}V_P}{\mathrm{d}t} = F_D(V - V_P) + g\frac{(\rho_P - \rho)}{\rho} + F \tag{3}$$

where $F_D(V - V_P)$ is the drag force of the discharge debris particles and its coefficient F_D is expressed as,

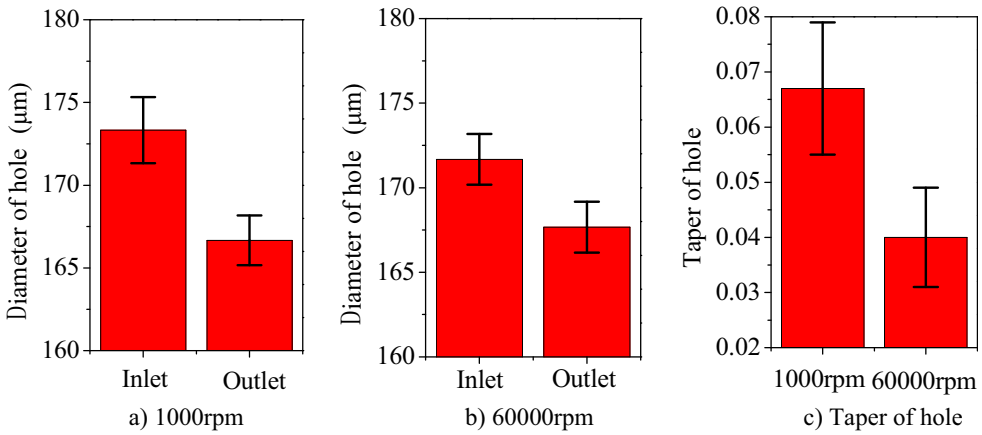

Fig. 8 Diameter of machined holes at the speed of 1000 rpm and 60,000 rpm

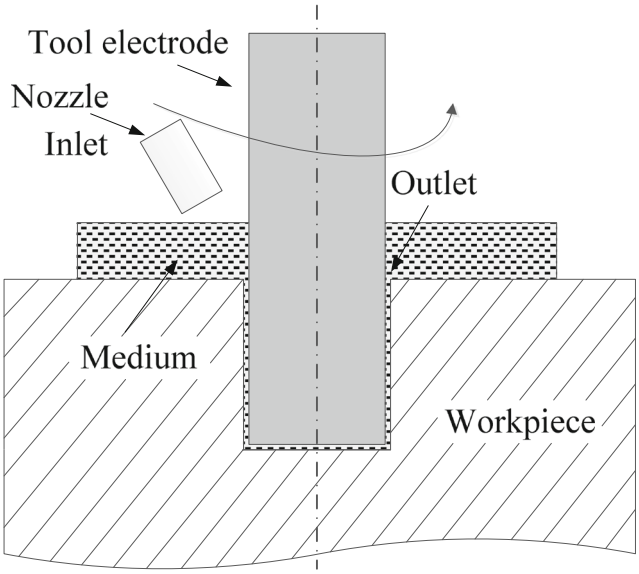

Fig. 9 Geometric model of micro hole machining

$$F_D = \frac{18\mu C_D R_e}{24 d_p^2 \rho_P} \tag{4}$$

where d_p is the diameter of the discharge chip, V_P is the discharge debris particles speed, ρ_P is the discharge debris particles density, $\mu$is the fluid dynamic viscosity, $C_D$is the drag coefficient, and R_e is the relative Reynolds coefficient of the discharge debris particles.

3.4 Setting of flow field model

In the model, the diameter of the tool electrode was Φ200 μm, the inlet pressure of the liquid was 0.1 MPa, the outlet pressure was 0, and the actual measured discharge gap was about 4 μm. In micro hole machining, the flow velocity of the medium was greatly influenced by side flushing and the high-speed rotation of the tool electrode, so the influence of turbulence on the flow field in the working gap was considered. Considering the computational efficiency of the model, a standard turbulence model $k-\varepsilon$ was selected.

Because the workpiece selected in the process of the experimental machining was tool steel, steel was selected as the material of the discharge debris particles. In order to facilitate the study, the selected diameter of discharge debris particle was set to Φ0.5 μm. The spray type of the discharge debris particles was chosen to spray from the surface, and the bottom of the model is jet surface according to the machining characteristics of micro holes. The initial velocity of discharge debris particles was (0,0,0), and the mass flow rate was the material removal rate of the workpiece, which was set at 5000 $\mu m^3/s$. Figure 10 shows the main surfaces of the working fluid in this model. In micro hole machining, the tool electrode is always in a rotating state while the workpiece is always in a stationary state. Therefore, the surface of the working fluid in contact with the electrode is set to a rotating wall, and the surface of the working fluid in contact with the workpiece is set to a stationary wall. The surface of the working fluid that is in contact with the air is set to a free surface, which is set to a symmetry condition. In the simulation, it is assumed that the collision between the discharge debris particles and the wall is elastic collision, and there is no energy loss in the collision process. In the experiment, the medium was kerosene, so kerosene-liquid was chosen as the physical property of the fluid.

3.5 Analysis of working gap flow field

3.5.1 Simulation results

Figure 11 shows the flow velocity cloud map at the location of B_1 and B_2 at A-A section at different rotational speeds. It can be seen that with the increase of the rotating speed of the tool electrode, the flow velocity of the medium in the B_1 position increases obviously. In the position of B_2, it is found that the velocity of the fluid in the side gap increases gradually as the rotating speed of the tool electrode increases.

Fig. 10 Main surface of model

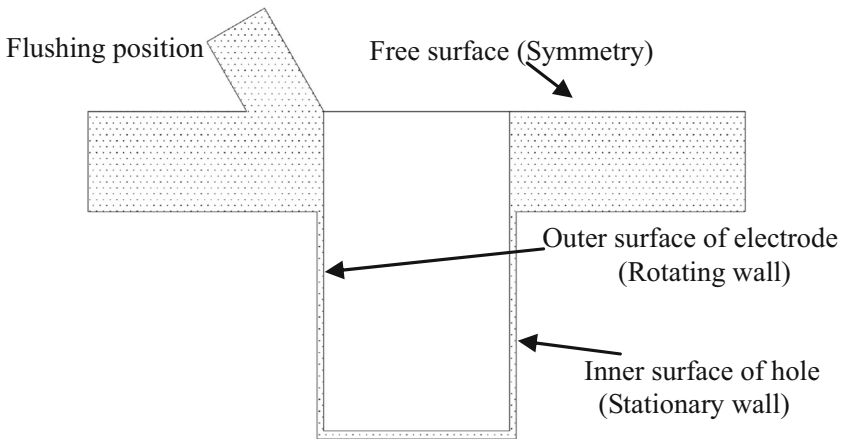

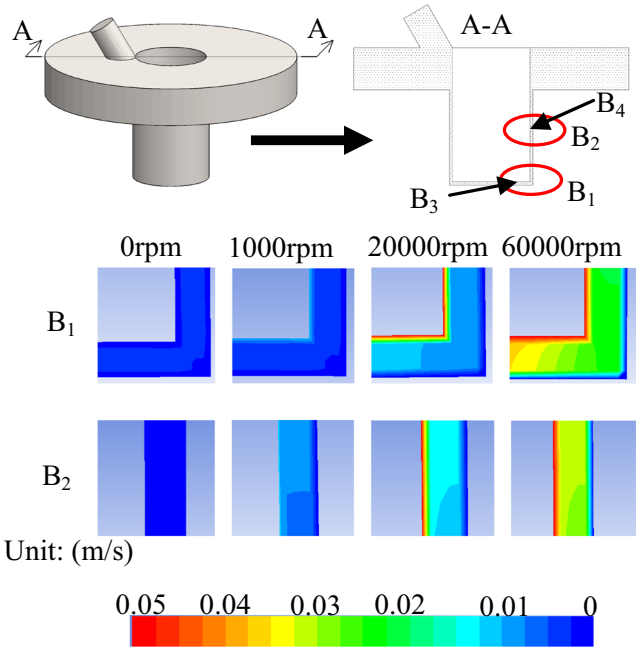

Fig. 11 Flow velocity distribution

Table 3 shows the velocity of the medium at the B_3. It can be seen that with the increase of the rotating speed of the tool electrode, the velocity of the B_3 along the axial direction of the tool electrode increases gradually.

Table 4 shows the velocity of the medium at the B_4. It can be seen that with the increase of the rotating speed of the tool electrode, the velocity of the B_4 along the axial direction of the tool electrode increases gradually.

Figure 12 shows the distribution of the discharge debris particles in the flow field after the simulation of 1 ms when the rotating speed of the tool electrode are 0 rpm, 1000 rpm, 20,000 rpm, and 60,000 rpm, respectively. When the rotating speed of the tool electrode is 0 rpm, the discharge debris particles are mainly concentrated at the bottom of the discharge gap due to the unrotation of the tool electrode. When the rotating speed of the tool electrode is increased to 1000 rpm, most of the discharge debris particles are still at the bottom, but a small part has entered into the side gap. When the rotating speed of the tool electrode reaches 20,000 rpm and 60,000 rpm, a large number of discharge debris particles have entered into the side gap from the bottom, and some of the discharge debris particles have gone from the side gap into the free liquid. This shows that higher tool electrode rotation can effectively remove debris particle in the gap between the tool electrode and the workpiece. The discharge debris particles remove rapidly from the gap, which can effectively reduce the occurrence of abnormal discharge in the working gap. The decrease in the probability of occurrence of abnormal discharge can improve the machining efficiency, reduce the electrode wear, and obtain micro holes with smaller taper in micro hole machining in EDM.

3.5.2 Analysis of debris in the bottom gap

From the above flow field simulation analysis, it can be seen that the bottom gap flow field has a velocity gradient. Therefore, the discharge debris particles are subjected to the Saffman force F_S, which is perpendicular to the direction of motion. Its calculation equation is as follows:

$$F_S = 1.61 d_p^2 (\rho\mu)^{1/2} (V - V_p) |dV/dy|^{1/2} \quad (5)$$

where, V is the velocity of the fluid, V_p is the velocity of the discharge debris particles, ρ is the density of the fluid, μ is fluid viscosity, d_p is the diameter of the discharge debris particles, and $|dV/dy|$ is the velocity gradient of the fluid.

In addition, since the fluid rotates with the tool electrode at a high speed, the debris is subjected to the drag force F_d of the fluid (the direction is consistent with the direction of the discharge debris velocity), and the expression is as follows:

$$F_d = 0.5 C_D A_p \rho (V - V_p)^2 \quad (6)$$

Since the flow field is turbulent, the drag coefficient C_D = 0.44. A_p is the projection of the debris on a plane perpendicular to the direction of motion. Since the discharge debris particles are spherical particles, so $A_p = 0.25\pi d_p^2$. Bring C_D and A_p into the Eq. (6) to get Eq. (7),

$$F_d = 0.055\pi\rho d_p^2 (V - V_p)^2 \quad (7)$$

Table 3 Velocity of B_3

Rotating speed (rpm)	Velocity of B_3 (m/s)	
	Total velocity	Velocity components along the Z axis
0	0.000623	0.00061
1000	0.00436	0.00144
20,000	0.0208	0.0079
60,000	0.0816	0.0213

Table 4 Velocity of B_4

Rotating speed (rpm)	Velocity of B_4 (m/s)	
	Total velocity	Velocity components along the Z axis
0	0.000183	0.00017
1000	0.00167	0.00055
20,000	0.00374	0.00142
60,000	0.0127	0.00332

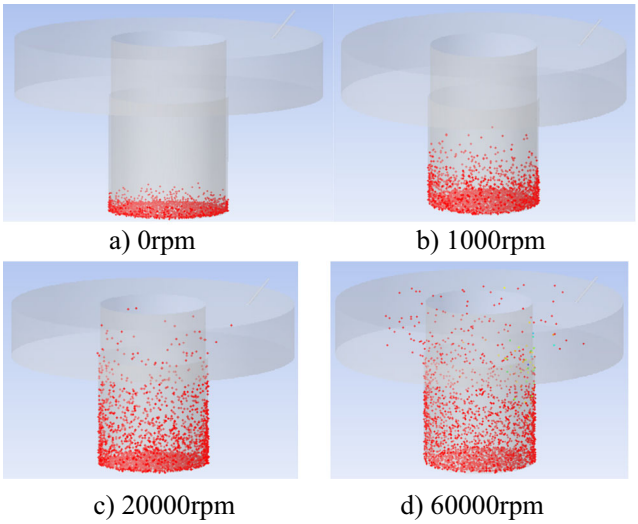

Fig. 12 Discharge debris particle distribution in the gap at different rotational speeds

Li et al. [21] and Alajbegovic et al. [22] showed that in the turbulent model, as the fluid flow velocity V increases, the value of $(V - V_p)$ gradually increases. Therefore, as the rotating speed of the tool electrode increases, the Saffman force F_s and the drag force F_d gradually increase. Since the bottom working gap fluid rotates as the electrode rotates, there is a velocity gradient along the axial and radial direction of the electrode. Therefore, the Saffman force F_s has components F_{s1} along the axial direction of the electrode and F_{s2} along the radial direction of the electrode. Because the discharge debris particles follow the flow of the fluid in the bottom gap, the drag force has components F_{d1} along the axial direction of the electrode and F_{d2} perpendicular to the A-A section. In addition to the above forces, the discharge debris particles are also affected by their own gravity mg and buoyancy F_f. Therefore, the force of the discharge debris particles in the bottom gap is shown in Fig. 13. In the figure, $F_1 = F_{s1} + F_{d1} + F_f$, $F_2 = F_{s2}$, $F_3 = mg$, $F_4 = F_{d2}$.

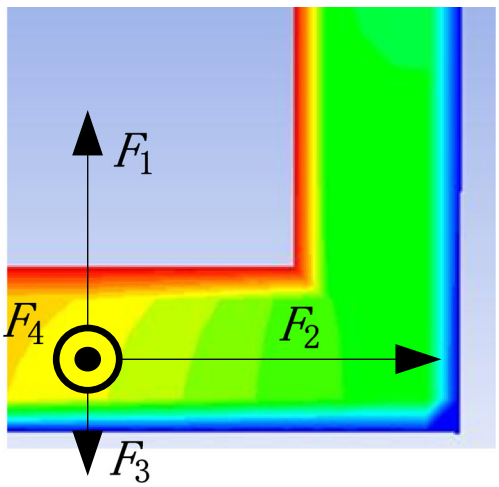

Fig. 13 Force diagram of discharge debris particles in the bottom gap

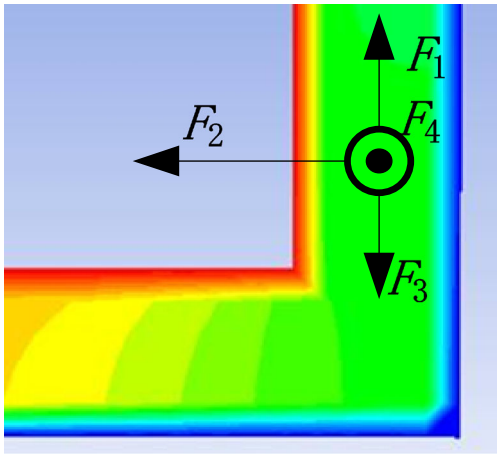

Fig. 14 Force diagram of discharge debris particles in the side gap

As the rotating speed increases, the Saffman force F_s and drag force F_d increase, and the values of F_1, F_2, and F_4 increase. Therefore, the difference between F_1 and F_3 increases, and the discharge debris particles move upward with the fluid. The resultant force between F_2 and F_4 increases, and the discharge debris particles are more likely to move away from the bottom gap. That is to say, by increasing the rotating speed of the tool electrode, the discharge debris particles in the bottom gap is more likely to enter the side gap and the velocity at the time of entering the side gap is greater.

3.5.3 Analysis of debris in the side gap

Since the side working gap fluid rotates as the electrode rotates, there is a velocity gradient along the radial direction of the electrode. Therefore, the Saffman force F_s is along the radial direction of the electrode. The drag force F_d has components F_{d1} along the axial direction of the electrode and F_{d2} perpendicular to the A-A section according to Table 4. Therefore, the force of the discharge debris particles in the side gap is shown in Fig. 14. In the figure, $F_1 = F_{d1} + F_f$, $F_2 = F_s$, $F_3 = mg$, $F_4 = F_{d2}$.

As the rotating speed increases, the Saffman force F_s and drag force F_d increase, and the values of F_1, F_2, and F_4 increase. Therefore, the difference between F_1 and F_3 increases, and the discharge debris particles move upward with the fluid. That is to say, by increasing the rotating speed of the tool electrode, the discharge debris particles in the side gap is more likely to remove from the side gap.

However, when the electrode rotation speed is less than 1000 rpm, the velocity component of the flow field in the vertical direction in the side gap is very small. Therefore, when the electrode rotation speed is low, the influence on the removal of the discharge debris particles is small. When the electrode rotation speed is 60,000 rpm, it can be seen from Table 4 that the velocity component in the vertical direction of the B_4 point in the side gap is about 20 times than when the

electrode rotation speed is 0 rpm. Therefore, the high electrode rotation speed is more favorable for removing the discharge debris particles from the side gap.

4 Conclusions

A micro hole machining experiment with different depth and the velocity field of the working gap medium and distribution of the discharge debris particles in the working gap were investigated at different rotating speeds of the tool electrode. Conclusions of this research are shown as follows:

- With the increase of the rotating speed, the material removal rate, the electrode wear ratio, and the taper of the machined holes would be improved.
- The higher rotating speed of the tool electrode had a better effect on improving the material removal rate and the electrode wear ratio during deeper hole machining.
- The flow field simulation results of micro hole machining at different rotating speeds of the tool electrode showed that the higher rotating speeds of the tool electrode were beneficial to the removal of the discharge debris particles from the gap and in improving the stability of the machining process in micro hole machining.

Funding information This research was financially supported by the National Natural Science Foundation of China (General Program, 51175121, 51575136) and the Key Project of Natural Science Foundation of Heilongjiang Province (ZD2015009).

References

1. Pham DT, Dimov SS, Bigot S, Ivanov A, Popov K (2004) Micro-EDM: recent developments and research issues. J Mater Process Technol 149(1):50–57
2. Zeng ZQ, Wang YK, Wang ZL, Shan DB (2012) Effect of dielectric medium on electrode wear in micro-electrical discharge milling. Nanotechnol Precis Eng 22(1):27–35
3. Kadirvel A, Hariharan P, Gowri S (2012) A review on various research trends in micro-EDM. Int J Mechatron Manuf Syst 5(5–6):361–384
4. Soni JS, Chakraverti G (1994) Machining characteristics of titanium with rotary electro-discharge machining. Wear 171(1–2):51–58
5. Cyril PJ, Asokan P, Jerald J, Kanagaraj G, Nilakantan JM, Nielsen I (2017) Tool speed and polarity effects in micro-EDM drilling of 316L stainless steel. Prod Manuf Res 5(1):99–117
6. Tong H, Li Y, Wang Y (2008) Experimental research on vibration assisted EDM of micro-structures with non-circular cross-section. J Mater Process Technol 208(1–3):289–298
7. Zhang QH, Zhang JH, Deng JX, Qin Y, Niu ZW (2002) Ultrasonic vibration electrical discharge machining in gas. J Mater Process Technol 129(1–3):135–138
8. Zhang QH, Zhang JH, Ren SF, Deng JX, Ai X (2004) Study on technology of ultrasonic vibration aided electrical discharge machining in gas. J Mater Process Technol 149(1–3):640–644
9. Masuzawa T, Heuvelman CJ (1983) A self-flushing method with spark-erosion machining. CIRP annals-Manuf Technol 32(1):109–111
10. Yan BH, Wang CC (1999) The machining characteristics of Al_2O_3/6061Al composite using rotary electro-discharge machining with a tube electrode. J Mater Process Technol 95(1–3):222–231
11. Meena VK, Azad MS, Mitra S (2012) Effect of flushing condition on deep hole micro-EDM drilling. Int J Mach Mach Mater 12(4):308–320
12. Zhao WS, Wang ZL, Di SC, Chi GX, Wei H (2002) Ultrasonic and electric discharge machining to deep and small hole on titanium alloy. J Mater Process Technol 120(1–3):101–106
13. Plaza S, Sanchez JA, Perez E, Gil R, Izquierdo B, Ortega N, Pombo I (2014) Experimental study on micro EDM drilling of Ti6Al4V using helical electrode. Precis Eng 38(4):821–827
14. Kumar R, Singh I (2018) Productivity improvement of micro EDM process by improvised tool. Precis Eng 51:529–535
15. Liu K, Lauwers B, Reynaerts D (2010) Process capabilities of micro-EDM and its applications. Int J Adv Manuf Technol 47(1–4):11–19
16. Zhang Y, Zhao H, Zhang G, Wang ZL, Zhao WS (2008) Research on a micro-EDM system and its techniques. China Mach Eng 19:526–530
17. Yang XD, Kimori M, Kunieda M, Araie I, Sano S (2007) Machining Properties of Micro EDM Using Electrostatic Induction Feeding. Proc ISEM XV:231–234
18. Yang X, Kunieda M, Sano S (2008) Study on influence of stray capacitance on micro EDM using electrostatic induction feeding. Int J Electr Mach 13:35–40
19. Koyano T, Kunieda M (2010) Achieving high accuracy and high removal rate in micro-EDM by electrostatic induction feeding method. Ann CIRP 59(1):219–222
20. Feng GL, Yang XD, Chi GX (2017) Study on machining characteristics of micro EDM with high spindle speed using non-contact electric feeding method. Int J Adv Manuf Technol 92(5–8):1979–1989
21. Li H, Xu WL, Li KF, Li J (2002) Study on particle diffusion coefficient of turbulent shear flow in open channel. J Hydraul Eng 33(8):47–52
22. Alajbegovic A, Drew DA, Lahey JRT (1999) An analysis of phase distribution and turbulence in dispersed particle/liquid flows. Chem Eng Commun 174(1):85–133